International Journal of Engineering

Characteristics of PANi/rGO Nanocomposite as Protective Coating and Catalyst in Dye-sensitized Solar Cell Counter Electrode Deposited on AISI 1086 Steel Substrate

N. Sofyan*[a,b], R. A. Nugraha[a], A. Ridhova[a], A. H. Yuwono[a,b], A. Udhiarto[c]

[a] Department of Metallurgical and Materials Engineering, Faculty of Engineering, Universitas Indonesia, Depok, Indonesia
[b] Tropical Renewable Energy Center, Faculty of Engineering, Universitas Indonesia, Depok, Indonesia
[c] Department of Electrical Engineering, Faculty of Engineering, Universitas Indonesia, Depok, Indonesia

P A P E R   I N F O

A B S T R A C T

One of the possibilities to mass-produce dye-sensitized solar cell (DSSC) device is if it could be embedded to the area atop metal roof. However, the use of metal substrate is constrained by the corrosion caused by the electrolyte solution used in the DSSC device such as iodide/tri-iodide ($I/I3_-$). In this study, we propose the utilization of polyaniline/reduced graphene oxide (PANi/rGO) nanocomposite as protective coating and at the same time as catalyst for the DSSC counter electrode on AISI 1086 steel substrates. The work was started by synthesizing PANi and rGO and assembling the PANi/rGO nanocomposite in a DSSC device. The characterization was performed using X-ray diffraction (XRD) for crystal structure, infrared (FTIR) for functional groups, scanning electron microscope (SEM) for surface morphology, potentiodynamic polarization and electrochemical impedance spectroscopy (EIS) for corrosion testing, and semiconductor parameter analyzer (SPA) for the DSSC device performance. The result showed that the decrease of corrosion rates in AISI 1086 steel was proportional to the rGO concentrations in PANi/rGO nanocomposites. The lowest corrosion rate was obtained at the highest rGO composition, i.e. PANi/rGO 8 wt% with corrosion rate (CR) of 0.2 mm/year and protection efficiency of 80.3 %. The DSSC performance test revealed that PANi/rGO composite could be used as an alternative catalyst for $I/I3_-$ based redox electrolyte in the DSSC solar cell applications in replacement for platinum. The highest power conversion efficiency of 5.38 % was obtained from PANi/rGO 4 wt%.

doi: 10.5829/ije.2018.31.10a.17

1. INTRODUCTION

Dye-sensitized solar cell has drawn the attention of many researchers because of its advantage in terms of low production cost and usage of cheap materials with abundant sources [1-4]. One of the possibilities to mass-produce of this dye-sensitized solar cell (DSSC) device is if it could be embedded to the area atop the metal roof. However, the use of metal substrate as a counter electrode in the DSSC device is constrained by the corrosion process resulted from electrolyte solution such as iodide/tri-iodide (($I^-/I3^{3-}$), which is common electrolyte used in the DSSC device. In order to effectively prevent corrosion on this substrate, the use of nanocomposite

material for protective coating as well as catalyst in the DSSC counter electrode is required.

Graphene is an allotrope of carbon consisting of carbon atom that creates a hexagonal structure with unique properties [56]. Graphene can be synthesized by processing graphite into single-layer sheets of graphene through chemical oxidation [7]. When the layers of oxidized graphite are exfoliated to form a few layers of carbon atoms like graphene, they are called graphene oxide (GO) [8]. This GO can be further reduced to graphene-like sheets by removing the oxygen-containing groups with the recovery of a conjugated structure called reduced graphene oxide (rGO) [9].

Polyaniline (PANi) is one of highly conductive and stable polymers widely studied due to its simple and cheap synthesizing process [10]. One of the simple

*Corresponding Author Email: nofrijon.sofyan@ui.ac.id (N. Sofyan)

methods in synthesizing PANi is through a chemical process [11]. Oxidation of chemical polymerization from aniline monomer into PANi can be done using oxidizing solution, such as ammonium persulfate, in an acidic atmosphere ($1 < pH \leq 3$) [12].

Because of their unique properties, PANi/graphene composites have been employed in many areas [13-19]. Several investigators have investigated the use of PANi/graphene composite as a catalyst in DSSC [13-15] in which addition of graphene in PANi matrix can increase conversion efficiency. The use of PANi/graphene composite as protective coating has also been investigated by many researchers [16-18] in which addition of graphene in low concentration (< 10 wt%) could increase the corrosion resistance of metals. However, combination of PANi/rGO nanocomposites have not been applied in development of DSSC device, specifically as protective coating and at the same time as catalyst in DSSC counter electrode deposited on AISI 1086 steel substrates.

In this work, the possibility of using PANi/rGO nanocomposite layer as protective coating and at the same time as an alternate catalyst for platinum replacement in the DSSC counter electrode deposited on AISI 1086 steel in electrolyte solution of I^-/I^{3-} was investigated and explored. The testing results from corrosion resistance of metals in redox electrolyte solution I^-/I^{3-} as well as the power conversion efficiency of the DSSC device were evaluated. Some of the results are presented and discussed in detail.

2. EXPERIMENTAL SETUP

2. 1. Preparation of PANi/rGO   Reduced graphene oxide (rGO) was synthesized from graphite by oxidizing it chemically using modification of Hummer method [20]. Graphite oxide formed was then ultra-sonicated for 120 minutes to form graphene oxide (GO). The GO was reduced to rGO via hydrothermal process using Zn as a catalyst [21]. The nanocomposite of PANi/rGO was synthesized via in situ polymerization method from aniline monomer with the help of oxidizing agent of ammonium persulfate in 0.5 M sulfuric acid [16].

2. 2. Deposition of PANi/rGO   The deposition of PANi/rGO layer was performed by dispersing 1 g of PANi/rGO in 50 mL mixture of ethanol and distilled water with a volume ratio of 2:1 and then was ultra-sonicated for 2 hours to obtain a homogenous mixture [15]. The PANi/rGO solution at different concentrations was drop-casted using a syringe on top of pre-cleaned AISI 1086 steel substrate before being dried at 80 °C. The result in the forms of thin PANi/rGO layer on the AISI 1086 steel substrate surface was ready for further treatment and characterization.

2. 3. Fabrication of DSSC   The DSSC device was fabricated by preparing the anode and the cathode. The cathode was prepared using different concentrations of PANi/rGO on pre-cleaned AISI 1086 steel substrate with a dimension of 2.5 cm x 2.5 cm. The anode was made using TiO_2 nanoparticle (Degussa P25) on an indium tin oxide (ITO) conductive glass substrate. TiO_2 nanoparticle was dissolved in ethanol and deposited on the surface of ITO glass by doctor blade method with a covered area of 1 cm x 1 cm. After the deposition process, the thin layer of TiO_2 was then sintered at 450 °C for 1 hour [22] to remove the solvent. The substrate was allowed to cool down to room temperature and was subsequently immersed in an organic dye sensitizer (RK-1, Solaronix) for 2 hours in a closed container and air-dried. Both of the anode and cathode substrates were attached to one another using binder clips at both ends separated by a spacer. Further, the electrolyte of I^-/I^{3-} made by mixing 0.5 M KI and 0.05 M I_2 in ethanol was injected in the gap between the electrodes. The DSSC device was then ready for characterization.

2. 4. Characterization   X-ray diffraction (XRD, ARL OPTX-2050) was carried out using Cu Kα radiation ($\lambda = 1.5406$ Å) at 40 kV and 35 mA to characterize the structural properties. Scanning electron microscope (SEM, JEOL JSM-6010) equipped with energy dispersive X-ray spectroscopy (EDX) was performed at 20 kV to characterize the surface morphology and elemental compositions. Electrochemical impedance spectroscopy (EIS, Autolab) was used to measure the potentiodynamic polarization according to ASTM G59 with three cells electrode, i.e. the working electrode (PANi/rGO nanocomposite coated AISI 1086 steel), the reference electrode (Ag/AgCl in 3 M KCl), and platinum as the auxiliary electrode. The DSSC device performance was characterized for its power conversion efficiency using semiconductor parameter analyzer (SPA, HP 4145B) with standard filter of AM 1.5 G and light intensity of 100 mW/cm^2 at room temperature.

3. RESULTS AND DISCUSSION

X-Ray diffraction patterns of pure PANi (PANi/rGO 0 wt%) and PANi/rGO nanocomposites at different concentrations are given in Figure 1. Diffraction peaks of pure PANi are at 2θ 14.56°, 20.28°, and 24.92° that correspond to the planes (200), (011) and (020), respectively. The diffraction pattern of PANi/rGO resembles to that of the pattern of pure PANi. Diffraction peak of rGO at 24.04° (plane 001) is no longer visible because it overlaps PANi diffraction peak. This shows that rGO sheets are enveloped by PANi particles in which rGO becomes polymerized and enclosed in PANi matrix homogenously [15].
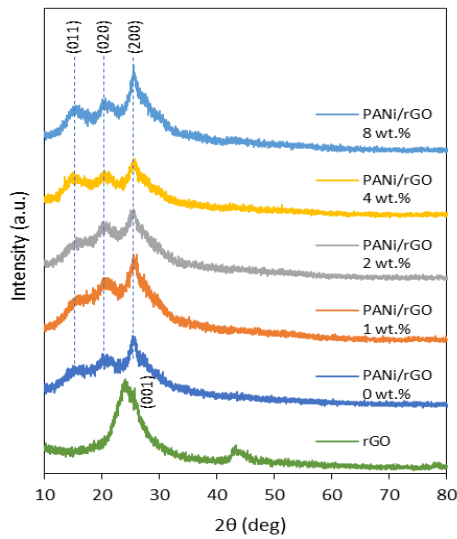
Figure 1. X-ray diffraction patterns of rGO and PANi/ rGO nanocomposites

The FTIR spectra results of pure PANi and PANi/rGO nanocomposites at rGO variation of 1, 2, 4, and 8 wt% are shown in Figure 2. For the pure PANi, the wavenumber of 3234 cm^{-1} shows absorption peak caused by N-H stretching from amine group. The absorption peak of C-H stretch is identified at wavenumber of 2919 cm^{-1}. At wavenumber of 1561 cm^{-1} and 1479 cm^{-1}, there are two sharp peaks identified as quinonoid and benzenoid ring stretching as the basic structure of PANi. The absorption peak caused by C-N stretching can be seen at wavenumber of 1286 cm^{-1}. At wavenumber of 1044 cm^{-1} there is an absorption peak of functional group HSO4^{-}/SO$_3^{-}$ where the dopant ion is sulfate or sulfite from the addition of H$_2$SO$_4$ 0.5 M during polymerization of PANi.
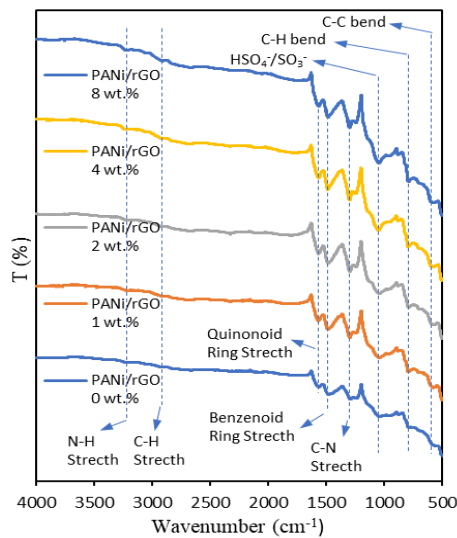

Figure 2. Infrared spectra of PANi/rGO nanocomposite

The wavenumbers range from 789 cm^{-1}, 575 cm^{-1} and 503 cm^{-1} are identified as absorption peaks caused by C-H, C-C and C-N-C bending [8, 23]. The absorption peak of PANi/rGO spectra resembles to that of the absorption peak of pure PANi.

The as-synthesized PANi/rGO nanocomposite deposited on AISI 1086 steel substrate was characterized for its morphology and chemical composition using SEM/EDX. The results are shown in Figure 3, whereas the chemical composition is tabulated in Table 1.
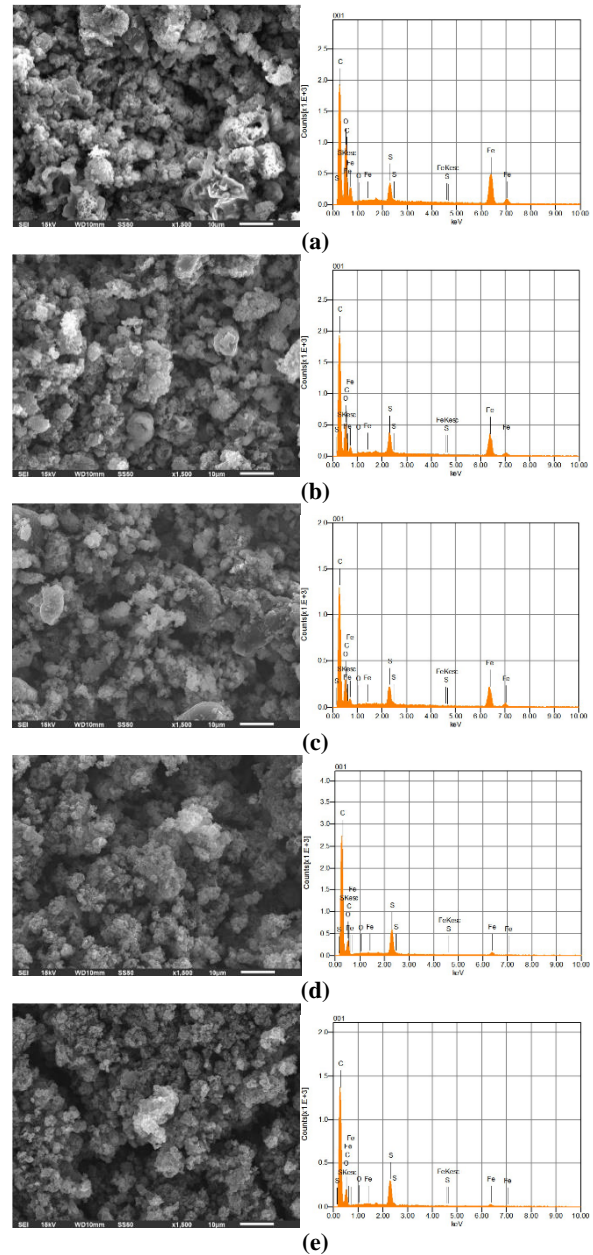

(a)

(b)

(c)

(d)

(e)

Figure 3. SEM/EDX results of PANi/rGO nanocomposite deposited on AISI 1086 substrate at rGO (a) 0 wt%, (b) 1 wt%, (c) 2 wt%, (d) 4 wt%, and (e) 8 wt%

TABLE 1. Identified elements of the EDX examination

| PANi/rGO Concentration	Identified Elements (wt%)			
	Fe	**C**	**O**	**S**
0 wt%	29.10	48.18	20.47	2.25
1 wt%	23.97	57.84	15.13	3.06
2 wt%	22.59	59.11	15.15	3.15
4 wt%	4.91	75.35	14.21	5.53
8 wt%	2.66	76.28	15.39	5.67

As seen in Figure 3, the surface morphology of PANi/rGO coating layer on AISI 1086 steel substrate shows particles agglomeration with distributed size. The elements identified from the chemical composition examination using EDX are iron (Fe) from the metal substrate, i.e. AISI 1086 steel; carbon (C) from the carbon chain in PANi (benzenoid and quinonoid rings) and the base structure of graphene/rGO; oxygen (O); and sulfur (S) representing the passive layer formed on the steel surface or ionic bond of SO_4^- on PANi, which is a dopant ion when synthesizing PANi with H_2SO_4 0.5 M solution. Addition of rGO to form PANi/rGO nanocomposite on the substrate causes the mass fraction of iron (Fe) and oxygen (O) to decrease and carbon (C) to increase. This also exhibits that the surface coverage of the steel substrate by PANi/rGO nanocomposite is becoming wide. Because of that, as seen in Table 1, it is understandable that the percentage of iron decreases with the increase of PANi/rGO concentration.

The presence of iron (Fe), oxygen (O), and sulfur (S) also indicates the formation of passive layer due to oxidizing reaction of the steel surface by PANi with H_2SO_4 0.5 M. The resulting passive layer could be $FeSO_4 \cdot 7H_2O$ or $FeSO_4 \cdot 4H_2O$ that is formed between the interface of the steel surface and the coating layer of PANi or PANi/rGO [24].

Electrochemical impedance spectroscopy (EIS) examination results are presented in the form of Nyquist curves. The curves are presented in Figure 4, whereas the equivalent electrical elements are given in Table 2. As seen in Figure 4, Nyquist curve of the AISI 1086 steel substrate with no coating is in the form of semicircle, whereas the coated one is in the form of linear curve with the slope is inversely proportional to the corrosion current density (i_{corr}).

The curve slope increases with the addition of more rGO concentration to the PANi/rGO nanocomposite, while the corrosion current decreases. This result agrees with the result found by other investigators [16].

According to the data, charge transfer resistance (Rct) or polarization resistance (Rp) and double layer capacitance (CDL), in each of PANi/rGO nanocomposite coating with rGO variations generally shows an increase in Rct or Rp value with an increase of rGO concentration, which indicates passivation on the steel substrate surface.
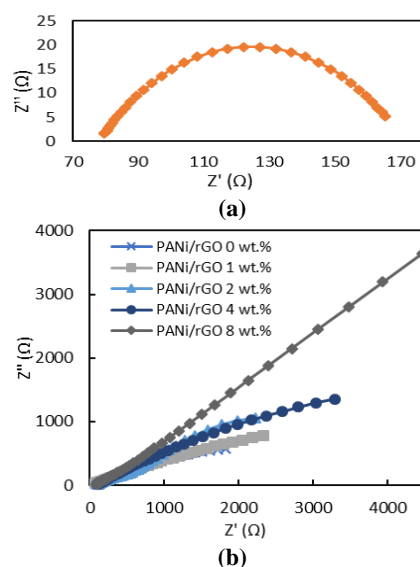
Figure 4. Nyquist curve of AISI 1086 with (a) no coating and (b) PANi/rGO at various compositions

TABLE 2. Equivalent electrical element value of EIS

Sample	Rs (Ω)	Rct/Rp (Ω)	Constant Phase Element	
			Y_0/CDL (μMho)	n
No coating	78.1	93	836	0.509
rGO 0 wt%	68.9	4240	662	0.344
rGO 1 wt%	20.8	10300	560	0.270
rGO 2 wt%	80.5	683	264	0.428
rGO 4 wt%	73.9	11400	438	0.358
rGO 8 wt%	73.7	1330	308	0.429

Other than that, decrease of CDL value means that the surface area covered by passive layer also increases.

On the surface of AISI 1086 steel coated by PANi/rGO nanocomposite, there is a potential shift to the positive direction compared to steel with no coating. This result agrees with SEM/EDX examination results in which the passive layer is formed due to the $FeSO_4$ reaction on metal surface after being coated using PANi and PANi/rGO.

The anodic Tafel slope (βa) value of the steel with PANi and PANi/rGO nanocomposite coating shows βa value lower than that of the steel with no coating in which the Tafel slope is almost flat. According to the calculated corrosion rate (CR) and i_{corr}, the higher rGO concentration, the more corrosion resistance. This confirms the passivation of steel by using PANi and PANi/rGO nanocomposite coating.

Protective coating efficiency of PANi/rGO is defined by Equation (1) given below [17, 18]:

$$P_{EF}(\%) = \frac{R_p(coated) - R_p(uncoated)}{R_p(coated)} \times 100\% \qquad (1)$$

Extrapolated Tafel results, log (i) vs E, can be seen detail in Table 3, which shows data of Tafel slopes for anodic and cathodic (βa and βc), corrosion potential (E$_{corr}$), corrosion current density (i$_{corr}$), polarization resistance (Rp), and corrosion rate (CR) in mm/year.

The protective coating efficiency of PANi/rGO nanocomposite at rGO concentration variations of 0, 1, 2, 4 and 8 wt% were 58.1, 76.7, 72.8, 71.2 and 80.3 %, respectively. It can be seen that the protective coating efficiency of PANi/rGO nanocomposite increases proportionally with the addition of rGO.

Impedance values in the forms of Bode modulus and phase curves are given in Figure 5.

TABLE 3. Electrochemical parameters of polarization test on PANi coated AISI 1086 at rGO composition variation

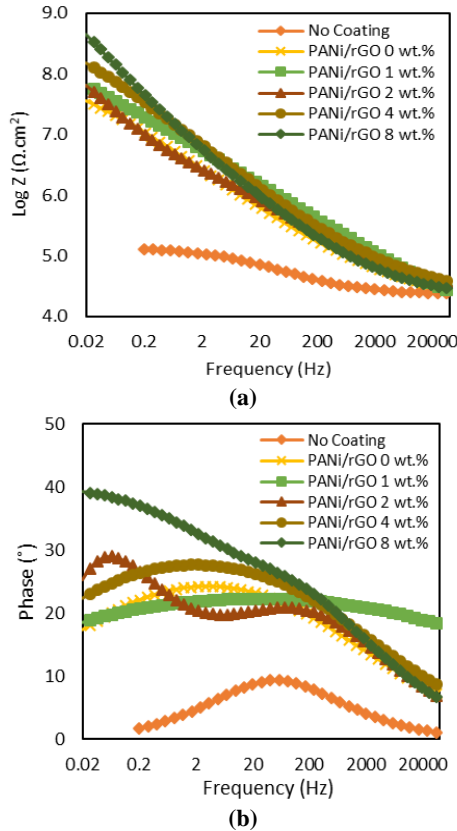| Sample	βa	βc	E$_{corr}$	i$_{corr}$	CR	R$_p$	P$_{EF}$ (%)
No coating	410.33	250.05	-236.62	149.81	1.74	450	-
Pure PANi	173.47	640.28	-228.51	55.13	0.64	1075	58.1
1 wt%	165.74	981.38	-82.98	31.82	0.37	1935	76.7
2 wt%	160.69	1836.70	-56.45	38.76	0.45	1656	72.8
4 wt%	126.07	646.23	-98.07	29.37	0.34	1560	71.2
8 wt%	101.04	1054.40	-32.95	17.57	0.20	2280	80.3

(a)

(b)

Figure 5. Bode modulus (a) and phase (b) curves

As seen in Figure 5, both Bode modulus and phase curves show that the impedance value from the steel with the use of pure PANi and PANi/rGO coating is higher than that of the steel with no coating. In according to impedance values, the higher the rGO concentration, the less the corrosion rate (CR). This result agrees with the results from potentiodynamic polarization test. Surface morphology of the samples was examined using SEM and the results are given in Figure 6. As seen in Figure 6, secondary electron images reveal PANi/rGO surface morphology that consists of PANi/rGO particles but some of them establish thick folds of passive layers.

The DSSC device performance was measured to explore the possibility of using PANi/rGO coated AISI 1086 steel (PANi/rGO-CS) as a counter electrode in comparison to the standard one using platinum on ITO substrate (Pt-ITO).
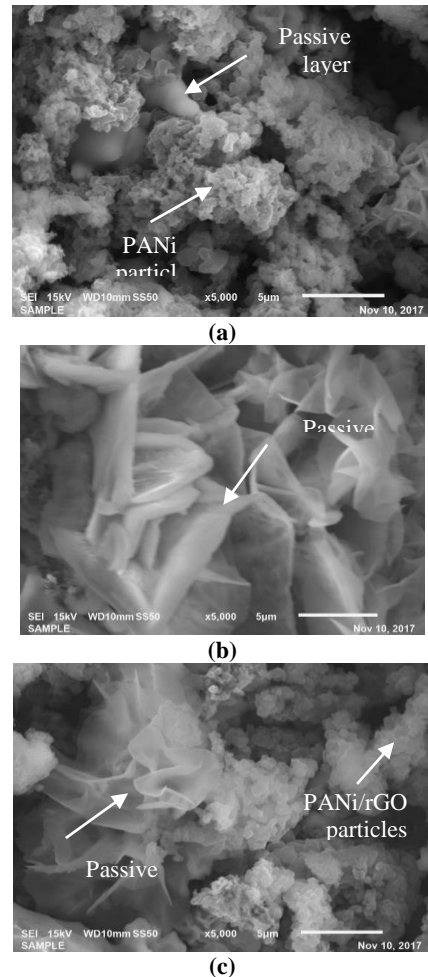
(a)

(b)

(c)

Figure 6. Secondary electron image of PANi/rGO surface morphology (a) Passive layer below PANi particles, (b) Passive layer in the form of thick folds in PANi/rGO 2 wt%, (c) Passive layer in the form of thick folds in PANi/rGO 8 wt%

The performance was measured in a way that when the DSSC device is exposed to a light, the power conversion efficiency (PCE, η) can be calculated from the short-circuit current (I_{SC}), open-circuit voltage (V_{OC}), fill factor (FF), and incoming light intensity (P_{IN}). In this instance, PCE is expressed by Equation (2).

$$\eta = \left(\frac{P_{MAX}}{P_{IN}} \right) = \left(\frac{V_{OC} \times I_{SC} \times FF}{P_{IN}} \right) \tag{2}$$

In this equation, Fill Factor (FF) is determined by Equation (3) [25]:

$$FF = \left(\frac{V_{MP} \times I_{MP}}{V_{OC} \times I_{SC}} \right) \tag{3}$$

where V_{MP} and I_{MP} values are voltage and maximum current density of the device, respectively, while P_{MAX} =$V_{MP} \times I_{MP}$ is the device maximum power.

The DSSC performance test in the forms of I-V curve is presented in Figure 7; whereas the DSSC efficiency parameter is given detail in Table 4. The curves and the parameters are used as comparison between the cathode using Pt-CS and the standard using Pt-ITO.

The DSSC device using Pt-ITO and Pt-CS electrodes shows a good performance proved by high I_{SC} value and thus the PCE. Although the DSSC device using Pt-ITO electrode has higher I_{SC} value as compared to that of using the platinum on AISI steel 1086 (Pt-CS), however, the DSSC device with Pt-CS has higher FF value than that of Pt-ITO resulting in nearly the same PCE value. On the contrary, the DSSC device with pure PANi as cathode (PANi/rGO 0 wt%-CS) results in low PCE because of low value of I_{SC}.

Further, the DSSC device with PANi/rGO nanocomposite at 1, 2, 4, 8 wt%-CS shows an increase in PCE values as compared to that of PANi/rGO 0 wt%-CS.
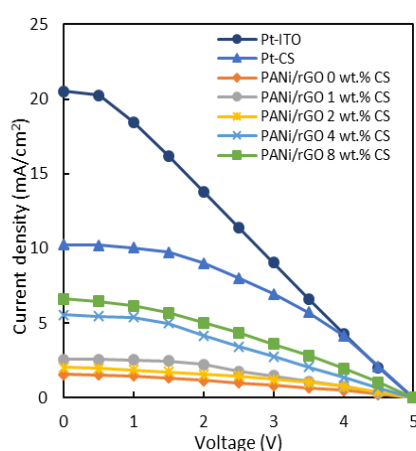
TABLE 4. Characteristics of the DSSC device using Pt and PANi at various rGO composition as counter electrodes

Substrate	Catalyst	DSSC Characteristics					
		V_{OC}	I_{SC}	V_{MP}	I_{MP}	FF	η (%)
ITO	Pt	5	20.52	0.5	20.24	0.10	10.12
	Pt	5	10.26	1	10.05	0.20	10.05
	0 wt%	5	1.55	1	1.46	0.19	1.46
AISI 1086	1 wt%	5	2.55	1.5	2.45	0.29	3.68
	2 wt%	5	2.02	1	1.85	0.18	1.85
	4 wt%	5	5.54	1	5.38	0.19	5.38
	8 wt%	5	6.62	0.5	6.47	0.10	3.23

In PANi/rGO 2 wt%-CS and PANi/rGO 8 wt%-CS, there is a decrease in PCE and I_{SC} values. This is possibly due to a decrease in surface contact area between PANi/rGO nanocomposite and reacting electrolyte of I^-/I^{3-} caused by passive layer enclosing PANi/rGO particles in the form of thick folds by size of > 20 μm as observed in Figure 6 of the secondary electron images. This may lead to decrease of the electrocatalytic performance of the DSSC device.

As seen in Table 4, for the AISI 1086 substrates, the highest PCE is obtained with PANi/rGO 4 wt%-CS nanocomposite coating with a PCE value of 5.38 %. Compared to the work of others, for examples PANi/Graphene Complex with a PCE of around 7 % [13], PANi/Graphene with a PCE of 6.09 % [15], PANi/GO with a PCE of 2.55 % [26], NiS anchored graphene/polyaniline nanocomposites with a PCE of around 5 % [27], and Ni–polyaniline–graphene with a PCE of around 5 % [28], this current PCE is still within the range and thus promising for the next development.

4. CONCLUSION

The synthesis of PANi and rGO nanocomposite as protective coating and at the same time as an alternate catalyst for platinum in the DSSC device was successfully carried out. The test results from potentiodynamic polarization and EIS showed that the decrease in corrosion rate is proportional to the rGO concentration in the PANi/rGO nanocomposite. The lowest corrosion rate was obtained from the highest rGO concentration at 8 wt% with a corrosion rate (CR) of 0.2 mm/year and protection efficiency of 80.3 %. The PANi/rGO nanocomposite coating has been proved to protect the AISI 1086 steel from I^-/I^{3-} electrolyte corrosion with passivation mechanism by preventing the corrosive ion to reach the steel surface (barrier effect). Performance conversion efficiency of the DSSC device showed that there is an increase of efficiency with the addition of PANi/rGO concentration. In this work, the

Figure 7. The I-V curve of the DSSC device using different catalyst on ITO and AISI 1086 steel (CS) substrates

highest PCE value was obtained from the DSSC device containing PANi/rGO nanocomposite at rGO concentration of 4 wt% with an efficiency of 5.38 %.

5. ACKNOWLEDGEMENT

6. REFERENCES

1. Xu, S., Liu, C., Wiezorek, J., "20 renewable biowastes derived carbon materials as green counter electrodes for dye-sensitized solar cells," *Materials Chemistry and Physics*, Vol. 204 (2018) 294-304.

2. Sofyan, N., Ridhova, A., Yuwono, A.H., and Udhiarto, A., "Fabrication of solar cells with TiO$_2$ nanoparticles sensitized using natural dye extracted from mangosteen pericarps", *International Journal of Technology*, Vol. 8, No. 7 (2017) 1229-1238.

3. Narayan, M.R., "Review: Dye Sensitized Solar Cells based on Natural Photosensitizers", *Renewable and Sustainable Energy Reviews*, Vol. 16, No. 1, (2012) 208-215.

4. Sofyan, N., Situmorang, F.W., Ridhova, A., Yuwono, A.H., and Udhiarto, A., "Visible light absorption and photosensitizing characteristics of natural yellow 3 extracted from Curcuma Longa L. for dye-sensitized solar cell", *IOP Conference Series: Earth and Environmental Science*, Vol. 105, (2018), 0120731-0120736.

5. Li, Z., Chen, L., Meng, S., Guo, L., Huang, J., Liu, Y., Wang, W., and Chen, X., "Field and temperature dependence of intrinsic diamagnetism in graphene: Theory and experiment", *Physical Review B*, Vol. 91, No. 9, (2015), 0944291-0944295.

6. Badiei, E., Sangpour, P., Bagheri, M., and Pazouki, M., "Graphene Oxide Antibacterial Sheets: synthesis and characterization, *IJE Transactions C: Aspects*, Vol. 27, No. 12, (2014), 1803-1808.

7. Emirua, T. F. and Ayele, D. W., "Controlled synthesis, characterization and reduction of graphene oxide: A convenient method for large scale production", *Egyptian Journal of Basic and Applied Sciences*, Vol. 4, No. 1, (2016), 74-79.

8. Novoselov, K.S., Geim, A.K., Morozov, S.V., Jiang, D., Zhang, Y., Dubonos, S.V., Grigorieva, I.V., Firsov, A.A., "Electric field effect in atomically thin carbon films", *Science*, Vol. 306, No. 5696, (2004), 666-669.

9. Pei, S., Cheng, H-M., "The reduction of graphene oxide", *Carbon*, Vol. 50, (2012), 3210-3228.

10. Wang, H., Lin, J., and Shen, Z.X., "Polyaniline (PANi) based electrode materials for energy storage and conversion", *Journal of Science: Advanced Materials and Devices*, Vol. 1, (2016), 225-255.

11. Stejskal, J., and Gilbert, R.G., "Polyaniline. Preparation of a conducting polymer", *Pure and Applied Chemistry*, Vol. 74, No. 5, (2002), 857-867.

12. Vadiraj, T. K. and Belagali, S., "Characterization of Polyaniline for Optical and Electrical Properties", *IOSR Journal of Applied Chemistry*, Vol. 8, No. 1, (2015), 53-56.

13. He, B., Tang, Q., Wang, M., Chen, H., and Yuan, S., "Robust Polyaniline–Graphene Complex Counter Electrodes for Efficient Dye-Sensitized Solar Cells", *ACS Applied Materials and Interfaces*, Vol. 6, No. 11, (2014), 8230-8236.

14. Jeong, G. H., Kim, S. J., Han, E. M., and Park, K. H., "Graphene/Polyaniline Nanocomposite Multilayer Counter Electrode by Inserted Polyaniline of Dye-Sensitized Solar Cells", *Molecular Crystals and Liquid Crystals*, Vol. 620, No. 1, (2015), 112-116.

15. Wang, G., Zhuo, S. and Xing, W., "Graphene/polyaniline nanocomposite as counter electrode of dye-sensitized solar cells", *Materials Letters*, Vol. 69, (2012), 27-29.

16. Cai, K., Zuo, S., Luo, S., Yao, C., Liu, W., Ma, J., Mao. H and Li, Z., "Preparation of polyaniline/graphene composites with excellent anti-corrosion properties and their application in waterborne polyurethane anticorrosive coatings", *RSC Advances*, Vol. 6 No. 98, (2016), 95965-95972.

17. Chang, C-H., Huang, T-C., Peng, C-W., Yeh, T-C., Lu, H-I, Hung, W-I, Weng, C-J., Yang, T-I, and Yeh, J-M., "Novel anticorrosion coatings prepared from polyaniline/graphene composites", *Carbon*, Vol. 50, No 14, (2012), 5044-5051.

18. Mahato, N. and Cho, M. H., "Graphene integrated polyaniline nanostructured composite coating for protecting steels from corrosion: Synthesis, characterization, and protection mechanism of the coating material in acidic environment", *Construction and Building Materials*, Vol. 115, (2016), 618–633.

19. Vaezi, M.R., Nikzad, L., and Yazdani, B., "Synthesis of CoFe$_2$O$_4$-polyaniline nanocomposite and evaluation of its magnetic properties", *International Journal of Engineering, Transactions B: Applications*, Vol. 22, No. 4, (2009), 381-386.

20. Zhou, T. N., Qi, X. D. and Fu, Q., "The preparation of the poly (vinyl alcohol)/graphene nanocomposites with low percolation threshold and high electrical conductivity by using the large-area reduced graphene oxide sheets", *Express Polymer Letters*, Vol. 7, No. 9, (2013), 747-755.

21. Liu, Y., Li, Y., Zhong, M., Yang, Y., Wen, Y., and Wang, M., "A green and ultrafast approach to the synthesis of scalable graphene nanosheets with Zn powder for electrochemical energy storage", *Journal of Materials Chemistry*, Vol. 21, (2011), 15449-15455.

22. Shanmugam, V., Manoharan, S., Anandan, S., Murugan, R., "Performance of dye-sensitized solar cells fabricated with extracts from fruits of ivy gourd and flowers of red frangipani as sensitizers", *Spectrochim Acta A*: Moleculer and Biomoleculer Spectroscopy, Vol. 104, (2013), 35-40.

23. Mostafaei, A. and Zolriasatein, A., "Synthesis and characterization of conducting polyaniline nanocomposites containing ZnO nanorods", *Progress in Natural Science: Materials International*, Vol. 22, No. 4, (2012), 273-280.

24. Sokolova, M. P., Smirnov, M. A., Kasatkin, I. A., Dmitriev, I. Y., Saprykina, N. N., Toikka, A. M., Lahderanta, E., and Elyashevich, G. K., "Interaction of Polyaniline with Surface of Carbon Steel", *International Journal of Polymer Science*, Vol. 2017, (2017), 1-9.

25. Jha, A. R., "Solar Cell Technology and Applications", Boca Raton: CRC Press Taylor and Francis Group, (2009).

26. Wang, M., Tang, Q., Chen, H., He, B., "Counter electrodes from polyaniline−carbon nanotube complex/graphene oxide multilayers for dye-sensitized solar cell application," *Electrochimica Acta*, Vol. 125 (2014) 510-515.

27. Nath, B.C., Mohan, K.J., Saikia, B.J., Ahmed, G.A., Dolui, S.K., "Designing of platinum free NiS anchored graphene/polyaniline nanocomposites-based counter electrode for dye sensitized solar cell," *Journal of Materials Science: Materials in Electronics*, Vol. 28, No. 1, (2017) 1042-1050.

28. Chen, X., Liu, J., Qian, K., Wang, J., "Ternary composites of Ni–polyaniline–graphene as counter electrodes for dye-sensitized solar cells," *RSC Advances*, Vol. 8, (2018) 10948-10953.

Characteristics of PANi/rGO Nanocomposite as Protective Coating and Catalyst in Dye-sensitized Solar Cell Counter Electrode Deposited on AISI 1086 Steel Substrate

N. Sofyan[a,b], R. A. Nugraha[a], A. Ridhova[a], A. H. Yuwono[a,b], A. Udhiarto[c]

[a] *Department of Metallurgical and Materials Engineering, Faculty of Engineering, Universitas Indonesia, Depok, Indonesia*
[b] *Tropical Renewable Energy Center, Faculty of Engineering, Universitas Indonesia, Depok, Indonesia*
[c] *Department of Electrical Engineering, Faculty of Engineering, Universitas Indonesia, Depok, Indonesia*

چکیده

یکی از امکاناتی که برای تولید سلولهای خورشیدی با حساسیت رنگی (DSSC) تولید می شود، این است که آیا می توان آن را به محفظه ای در پشت سقف فلزی جاسازی کرد. با این حال، استفاده از بستر فلزی توسط خوردگی ناشی از محلول الکترولیت مورد استفاده در دستگاه DSSC مثل یدید/تریدید (‏‏I/I3.) محدود شده است. در این مطالعه، استفاده از نانوکامپوزیت گرافین پلی آنیلین / کاهش گرافیتی (PANi / rGO) را به عنوان پوشش محافظتی و در همان زمان به عنوان کاتالیزور برای الکترود ضد DSSC در زیرزمین فولاد AISI 1086 پیشنهاد می کنیم. این کار با تلفیق PANi و rGO و جمع آوری نانوکامپوزیت PANi / rGO در یک دستگاه DSSC آغاز شد. مشخصه ها با استفاده از پراش اشعه ایکس (XRD) برای ساختار کریستال، مادون قرمز (FTIR) برای گروه های کاربردی، میکروسکوپ الکترونی اسکن (SEM) برای مورفولوژی سطح، پلاریزاسیون پتانسیودینامیکی و طیف سنجی امپدانس الکتروشیمیایی (EIS) برای آزمایش خوردگی و پارامتر نیمه هادی تجزیه کننده (SPA) برای عملکرد دستگاه DSSC. نتایج نشان داد که کاهش میزان خوردگی فولاد AISI 1086 متناسب با غلظت rGO در نانوکامپوزیتهای PANi / rGO بود. کمترین میزان خوردگی در بالاترین ترکیب rGO بدست آمد، به عنوان مثال ٪wt 8 rGO / PANi با نرخ خوردگی (CR) ۰/۲ میلی متر در سال و راندمان حفاظت ۸۰/۳ درصد است. تست عملکرد DSSC نشان داد که کامپوزیت PANi / rGO می تواند به عنوان یک کاتالیزور جایگزین برای الکترولیت Redox بر اساس ‏‏I/I3. در DSK های سلول خورشیدی در جایگزینی پلاتین استفاده شود. بیشترین بازده تبدیل قدرت از ٪۵/۳۸ از ٪wt 4 rGO / PANi بدست آمد.

doi: *10.5829/ije.2018.31.10a.17*